Spatial pattern formation of a ratio-dependent predator–prey model*

Lin Wang(林 望)†

College of Mathematics and Information Science, Wenzhou University, Wenzhou 325035, China

(Received 28 October 2009; revised manuscript received 24 December 2009)

This paper presents a theoretical analysis of evolutionary process that involves organisms distribution and their interaction of spatially distributed population with diffusion in a Holling-III ratio-dependent predator–prey model, the sufficient conditions for diffusion-driven instability with Neumann boundary conditions are obtained. Furthermore, it presents novel numerical evidence of time evolution of patterns controlled by diffusion in the model, and finds that the model dynamics exhibits complex pattern replication, and the pattern formation depends on the choice of the initial conditions. The ideas in this paper may provide a better understanding of the pattern formation in ecosystems.

Keywords: ratio-dependent predator–prey model, Holling III functional response, diffusion-driven instability, pattern formation

PACC: 0290, 0565

1. Introduction

The issue of spatial and spatio-temporal pattern formation in biological communities is probably one of the most exciting problems in modern biology and ecology. Promulgated by the theoretical paper of Turing,[1] the interplay of nonlinear reactions and diffusion has been regarded as the driving force of the spontaneous emergence of spatial structure in a variety of nonequilibrium situations.[2−4] Spatial component of ecological interactions has been identified as an important factor in how ecological communities are shaped.[5−8]

On the other hand, ratio-dependent predator–prey models[5,7−13] are increasingly favored by both the theoretical and experimental ecologists as a more suitable alternative to describe predator–prey interactions when the predators hunt seriously, especially those with Holling III functional response.[14−17] Thus, in this paper, we mainly focus on the following spatially extended ratio-dependent predator–prey model with Holling III functional response:

$$\begin{aligned}\frac{\mathrm{d}N}{\mathrm{d}t} &= rN\left(1-\frac{N}{k}\right)-\frac{aN^2}{N^2+m^2P^2}P+D_1\nabla^2 N,\\ \frac{\mathrm{d}P}{\mathrm{d}t} &= P\left(\frac{bN^2}{N^2+m^2P^2}-d\right)+D_2\nabla^2 P,\end{aligned}\tag{1}$$

where N and P are the prey and the predator densities, respectively. $r>0$ represents the intrinsic growth rate of the prey, $k>0$ is the carrying capacity of the prey in the absence of predator, $d>0$ is the death rate of the predator, D_1 and D_2 are the diffusion coefficients for N and P respectively, $\nabla^2=\partial/\partial N^2+\partial/\partial P^2$ is the usual Laplacian operator in two-dimensional space.

We consider the Neumann boundary conditions given by

$$\frac{\partial N}{\partial \nu}=\frac{\partial P}{\partial \nu}=0,$$

and initial conditions

$$\begin{aligned}&N(x,y,0)>0,\quad P(x,y,0)>0\\ &(x,y)\in\Omega=[0,R]\times[0,R],\end{aligned}$$

here, Ω is a bounded domain, $\partial N/\partial\nu$ and $\partial P/\partial\nu$ are respectively the normal derivatives of N and P on $\partial\Omega$. The main reason for choosing such boundary conditions is that we are interested in the self-organisation of pattern, and that Neumann boundary conditions imply no external input.

The aim of this paper is to study the spatiotemporal complexity of a diffusive ratio-dependent predator–prey model with Holling III functional response. The paper is organised as follows. In Section 2, we consider the equilibria of the model and their local stability. While in Section 3, we explore under what parameter values the diffusion-driven instability can occur. In Section 4, we give the spatial pattern formation via numerical simulation, i.e., the evolution process of the

*Project supported by the Natural Science Foundation of Zhejiang Province of China (Grant No. Y7080041).

†Corresponding author. E-mail: linwang@wzu.edu.cn

© 2010 Chinese Physical Society and IOP Publishing Ltd

system near the coexistence equilibrium point, and we perform a special perturbed initial condition to the coexistence equilibrium point to illustrate the emergence of spatiotemporal patterns. In the last section, some discussions and remarks are given.

2. Local stability analysis

In order to minimise the number of parameters involved in the model, it is extremely useful to write the system in non-dimensionalised form. Although there is no unique method of doing this, it is often a good idea to relate the variables to some key relevant parameters.[18] With $u = N/k$, $v = mP/k$, $t' = rt$, and t is used to represent t', we can arrive at the following equations containing dimensionless quantities:

$$\begin{aligned}\frac{\mathrm{d}u}{\mathrm{d}t} &= u(1-u) - \frac{\alpha u^2 v}{u^2+v^2} + \sigma\nabla^2 u,\\ \frac{\mathrm{d}v}{\mathrm{d}t} &= \frac{\beta u^2 v}{u^2+v^2} - \gamma v + \nabla^2 v,\end{aligned} \tag{2}$$

where $\alpha = a/rm$, $\beta = b/r$, $\gamma = \mathrm{d}/r$, $\sigma = D_1/D_2$.

Then we consider the equilibria and their local stability of the model Eq. (2) without diffusion. This information will be crucial in the next section where we study the effect of the relative diffusion coefficent on the stability of the steady states. In such a case the model reduces to

$$\begin{aligned}\frac{\mathrm{d}u}{\mathrm{d}t} &= u(1-u) - \frac{\alpha u^2 v}{u^2+v^2},\\ \frac{\mathrm{d}v}{\mathrm{d}t} &= \frac{\beta u^2 v}{u^2+v^2} - \gamma v.\end{aligned} \tag{3}$$

It can be seen that the model Eq. (3) has three nonnegative real equilibria:

(i) the equilibrium point $E_0 = (0,0)$ always exists and it is a saddle point with unstable manifold locally in the u-direction and with stable manifold locally in the v-direction;

(ii) the equilibrium point $E_1 = (1,0)$ corresponding to extinction of the predator is a saddle point with stable manifold locally in the u-direction and with unstable manifold locally in the v-direction when $\beta > \gamma$, or is locally asymptotically stable in the uv-plane when $\beta < \gamma$;

(iii) the non-trivial equilibrium point $E^* = (u^*, v^*)$ corresponds to coexistence of prey and predator, where

$$u^* = \frac{\beta - S}{\beta}, \qquad v^* = \frac{Su^*}{\alpha\gamma}. \tag{4}$$

It is easy to obtain that the conditions ensuring the positiveness of u^* and v^* are $\beta - \gamma > 0$ and $\beta - S > 0$, where $S = \sqrt{\alpha^2\beta\gamma - \alpha^2\gamma^2}$.

The Jacobian matrix of the linearized system of the model Eq. (3) at E^* is

$$\boldsymbol{J} = \begin{bmatrix} \dfrac{-\beta^2 + 2\gamma S}{\beta^2} & \dfrac{\alpha\gamma(\beta - 2\gamma)}{\beta^2} \\ \dfrac{2(\beta-\gamma)S}{\alpha\beta} & -\dfrac{2\gamma(\beta-\gamma)}{\beta} \end{bmatrix} \equiv \begin{bmatrix} a_{11} & a_{12} \\ a_{21} & a_{22} \end{bmatrix}. \tag{5}$$

The characteristic equation is

$$\lambda^2 - \mathrm{tr}(\boldsymbol{J})\lambda + \det(J) = 0, \tag{6}$$

where

$$\begin{aligned}\mathrm{tr}(\boldsymbol{J}) &= \frac{2\gamma S - \beta^2 - 2\beta^2\gamma + 2\beta\gamma^2}{\beta^2},\\ \det(\boldsymbol{J}) &= \frac{2\gamma(\beta-\gamma)(\beta - S)}{\beta^2},\end{aligned}$$

then, by Routh–Hurwitz criteria,[19] E^* is locally asymptotically stable in the uv-plane provided $\mathrm{tr}(\boldsymbol{J}) < 0$ and $\det(\boldsymbol{J}) > 0$ which gives $2\gamma S - \beta^2 - 2\gamma\beta^2 + 2\beta\gamma^2 < 0$, and $\beta > \gamma$. It may be noted here that under these conditions, the predator and prey species coexist, and they settle down at its equilibrium level.

3. Diffusion driven instability

In this section, we will derive conditions for the instability of the equilibrium point E^* by using Turing's technique.[20,1] Instability will occur due to diffusion when a parameter varies slowly in such a way that a stability condition is suddenly violated and it can bring about a situation wherein perturbation of a non-zero (finite) wavelength starts growing (perturbations of zero wave number are stable when diffusive instability sets in). To study the effect of diffusion on the system, we have considered the linearized form of Eq. (2) about E^* as follows:

$$\begin{aligned}\frac{\mathrm{d}U}{\mathrm{d}t} &= a_{11}U + a_{12}V + \sigma\nabla^2 u,\\ \frac{\mathrm{d}V}{\mathrm{d}t} &= a_{21}U + a_{22}V + \nabla^2 v,\end{aligned} \tag{7}$$

where $u = u^* + U$, $v = v^* + V$, and $a_{ij}, i, j = 1, 2$ are defined in Eq. (5). It may be noted that (U, V) are small perturbations of (u, v) about the equilibrium point E^*.

Equation (7) can be solved by separation of variables and expanding u and v in spatial Fourier series. Assume that

$$\begin{pmatrix} U \\ V \end{pmatrix} = \begin{pmatrix} A \\ B \end{pmatrix} \exp(\lambda t + \mathrm{i}\, kx).$$

where λ and k are the frequency and wave number respectively. The characteristic equation of the linearized system is given by

$$\lambda^2 - \rho_1 \lambda + \rho_2 = 0, \tag{8}$$

where the coefficients ρ_1 and ρ_2 are given by

$$\rho_1 = \mathrm{tr}(J) - (\sigma + 1)k^2,$$
$$\rho_2 = \det(J) - (a_{11} + a_{22}\sigma)k^2 + \sigma k^4.$$

To have diffusion-driven instability, at least one of the conditions $\rho_1 < 0$ and $\rho_2 > 0$ must be violated by Routh–Hurwitz criterion.[19] It is evident that the first condition $\rho_1 < 0$ is not violated when the condition $\mathrm{tr}(\boldsymbol{J}) < 0$ is met. Hence only the violation of condition $\rho_2 > 0$ gives rise to diffusion-driven instability. Thus, the condition for diffusion-driven instability is given by

$$H(k^2) = \sigma k^4 - (a_{11} + a_{22}\sigma)k^2 + \det(\boldsymbol{J}) < 0. \tag{9}$$

If the minimum of the function $H(k^2)$ is negative, then a range of modes $k_-^2 < k^2 < k_+^2$ will grow where

$$k_-^2 = \frac{(a_{11} + a_{22}\sigma) - \sqrt{(a_{11} + a_{22}\sigma)^2 - 4\sigma \det(\boldsymbol{J})}}{2\sigma}, \tag{10}$$

$$k_+^2 = \frac{(a_{11} + a_{22}\sigma) + \sqrt{(a_{11} + a_{22}\sigma)^2 - 4\sigma \det(\boldsymbol{J})}}{2\sigma}. \tag{11}$$

It is easy to check that

$$H_{\min} = \det(J) - \frac{(a_{11} + a_{22}\sigma)^2}{4\sigma} \tag{12}$$

occurs at

$$k^2 = \frac{(a_{11} + a_{22}\sigma)}{2\sigma}. \tag{13}$$

In particular, we have

$$\rho_2 < 0 \Longleftrightarrow k_-^2 < k^2 < k_+^2. \tag{14}$$

If both k_-^2 and k_+^2 exist and have positive values, they limit the range of instability for a local stable equilibrium (Fig. 1).

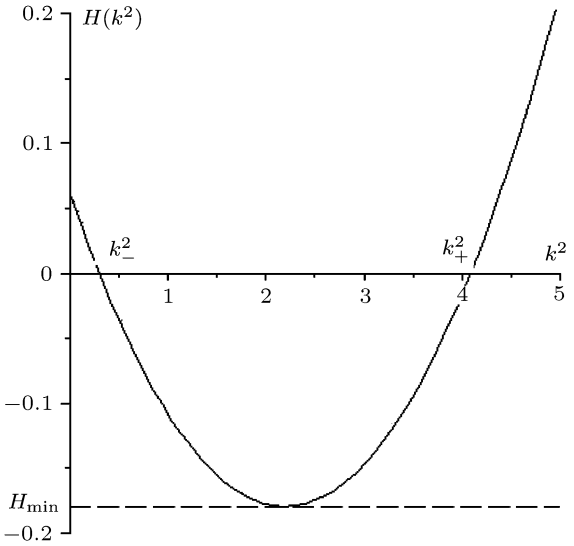


Fig. 1. Modes with wavenumbers lying between the zeros of $H(k^2)$, k_-^2 and k_+^2, grow in the Turing instability. Parameters: $\alpha = 2.2$, $\beta = 1$, $\gamma = 8/9$, $\sigma = 0.05$, hence, $k_-^2 = 0.2982471252$, $k_+^2 = 4.0870947$, and $H_{\min} = -0.1794420829$.

4. Pattern formation

We have shown in the above section that the non-trivial homogeneous stationary state can loose its stability when diffusion is taken into consideration. The diffusion-driven instability can appear within certain parameter spaces.[21] If the parameters are chosen appropriately the numerical simulations will give rise to strikingly rich and surprisingly beautiful two-dimensional patterns.[7]

In this section we perform numerical simulations to illustrate the results obtained in previous sections. Computer experiments are done in two-dimensional space with a square numerical domain $L \times L$. We solve the reaction–diffusion equations by using finite-difference approximation for the time integration. Neumann boundary conditions are employed in most calculations. And the steps Δh and Δt of the numerical grid are chosen sufficiently small so that the results are independent of the step size.

Since both species exhibit qualitatively similar behaviour, only the prey abundance is shown here. We run the simulations until the system goes into a time dependent state, or to an essentially steady state. Figure 2 shows the evolution of the spatial pattern of prey at $t = 0, 50, 500, 5000$ with small random perturbation

of the stationary solution E^* of the spatially homogeneous systems, the values of the parameters are that $\alpha = 2.05$, $\beta = 1$, $\gamma = 8/9$, $\sigma = 0.05$, and we choose $\Delta h = 1/3$, $\Delta t = 1/40$, $L = 100$. After irregular transient pattern, we observe that the stationary internal spatial resonance patterns with blue-eyes remain time independent finally, for more details, see Ref. [22]. This structure is emergent and arises from very simple causes, in the sense that it is macroscopic pattern emerging from simple coupling interaction and local diffusion rules. In other words, under this situation, spatially uniform steady-state predator–prey coexistence is no longer substained. Small random fluctuations will be strongly amplified by diffusion, leading to nonuniform population distributions.

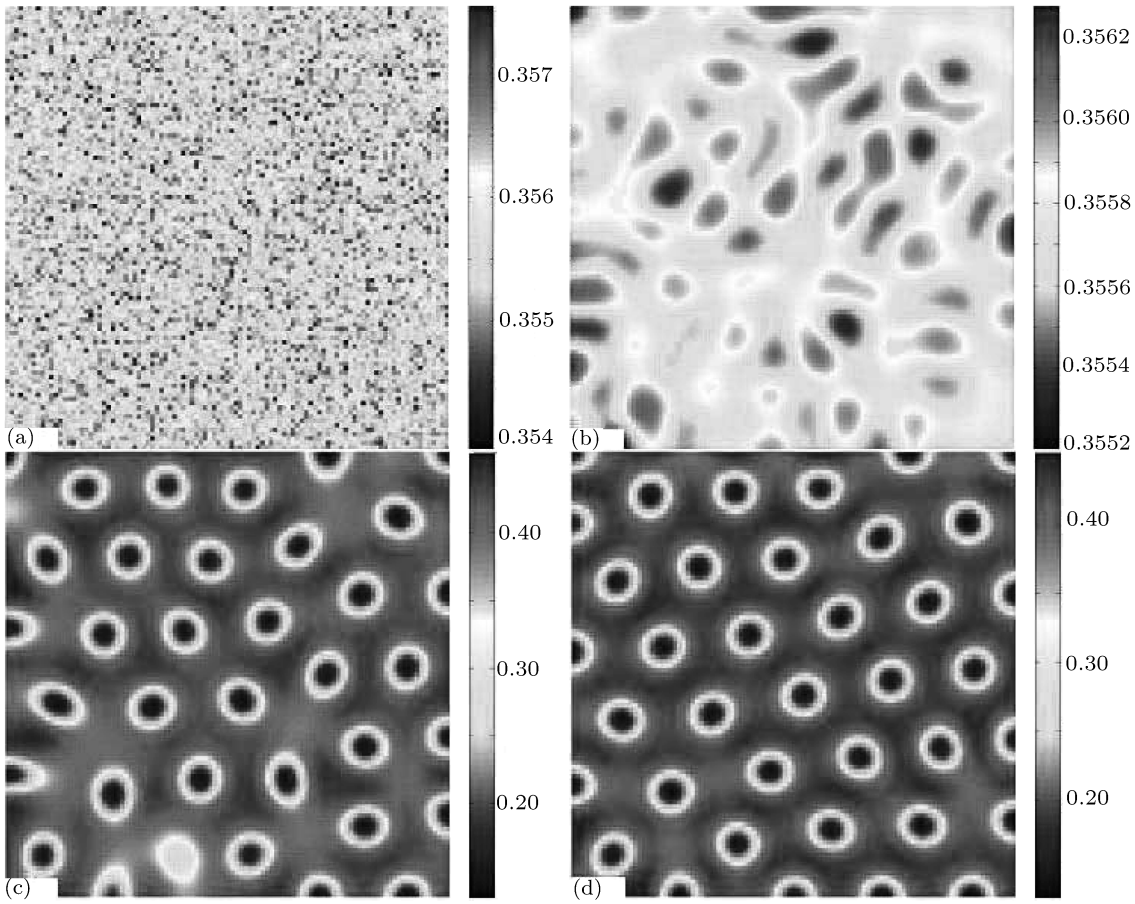


Fig. 2. Snapshots of contour pictures of the time evolution of the prey at different instants with $\alpha = 2.05$, $\beta = 1$, $\gamma = 8/9$, $\sigma = 0.05$: (a) $t = 0$; (b) $t = 50$; (c) $t = 500$; (d) $t = 5000$.

However, increasing α to 2.2 and keeping other parameters fixed, we find that the blue-eye patterns and the stripelike patterns coexist in the spatially extended model (c.f., Fig. 3(d)). If we vary α to 2.23, another spatial resonant pattern with twinkling blue-eyes arises as shown in Fig. 4, in which the shape of the blue-eyes is periodically changed. For the sake of learning this resonant behaviour further, we illustrate the temporal evolution process of prey density u in Fig. 5. Obviously, the system gives rise to periodic oscillations in time finally. In addition, Fig. 6 shows that a time-dependent irregular spiral pattern appears and prevails over the whole domain finally when $\alpha = 2.5, \sigma = 0.7$, and $L = 200$ for making the image more clearly. Comparing Fig. 2(d) with Figs. 3(d), 4 and 6(d), we can find that those patterns are quite different on account of the variation of α and σ.

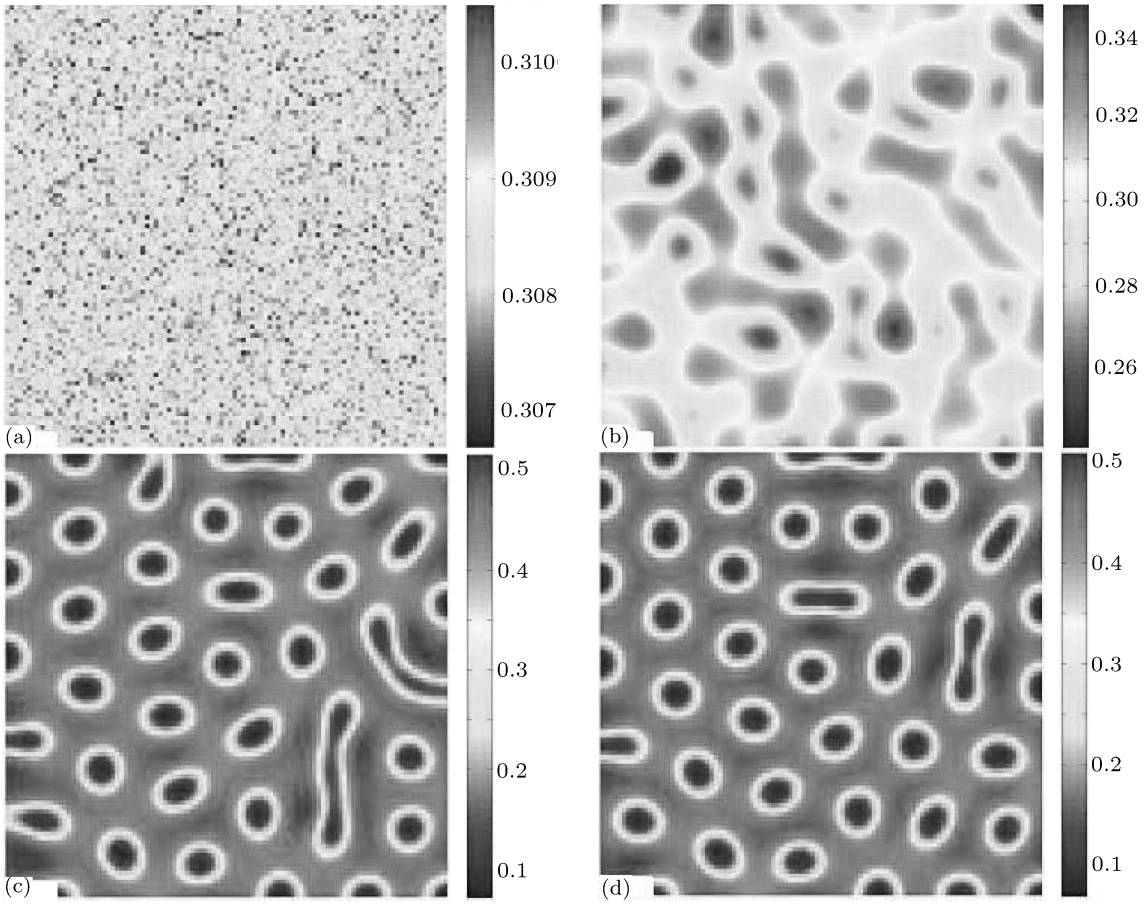


Fig. 3. Snapshots of contour pictures of the time evolution of the prey at different instants with $\alpha = 2.2$, $\beta = 1$, $\gamma = 8/9$, $\sigma = 0.05$: (a) $t = 0$; (b) $t = 50$; (c) $t = 500$; (d) $t = 5000$.

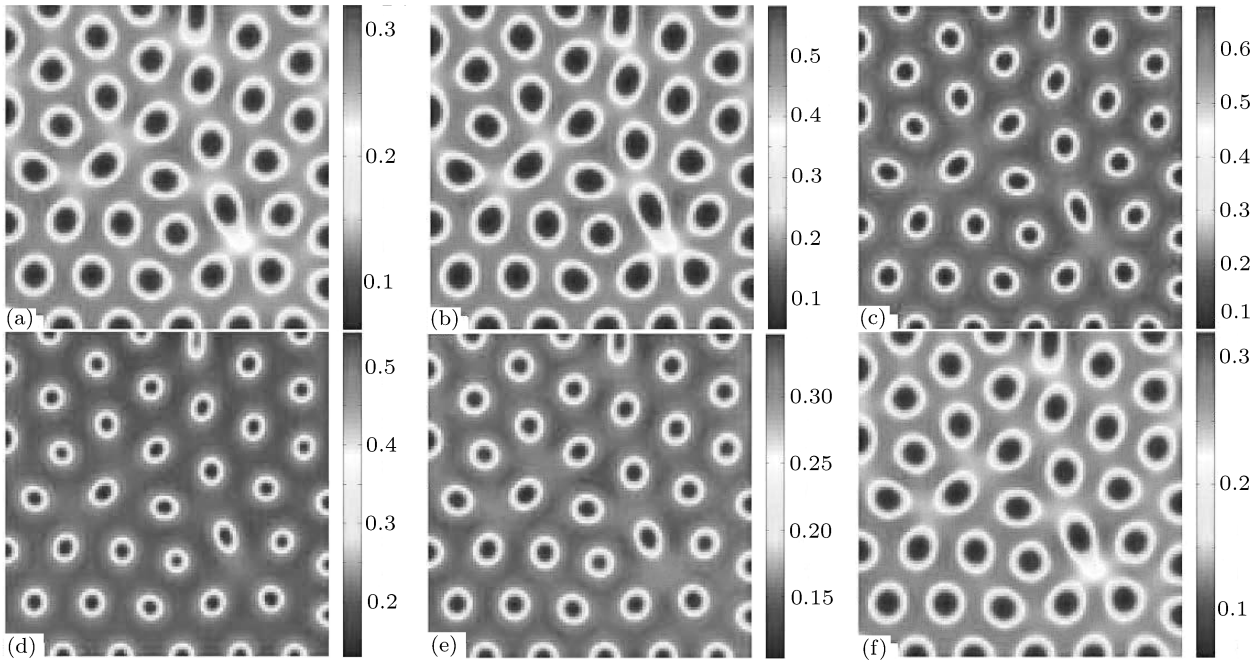


Fig. 4. Snapshots of contour pictures of the time evolution of the prey at different instants with $\alpha = 2.23$, $\beta = 1$, $\gamma = 8/9$, $\sigma = 0.05$: (a) $t = 4968$; (b) $t = 24867/5$; (c) $t = 24894/5$; (d) $t = 24921/5$;(e) $t = 24948/5$; (f) $t = 4995$.

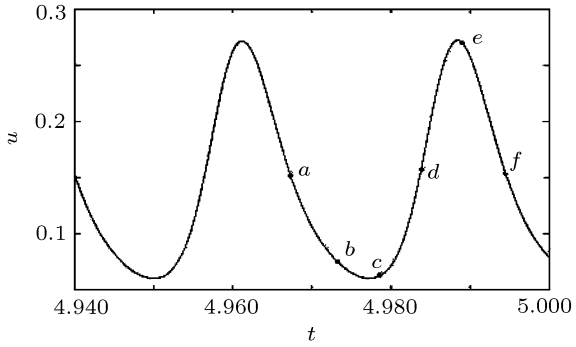


Fig. 5. The time-series of u corresponding to the snapshots of the patterns in Fig. 4.

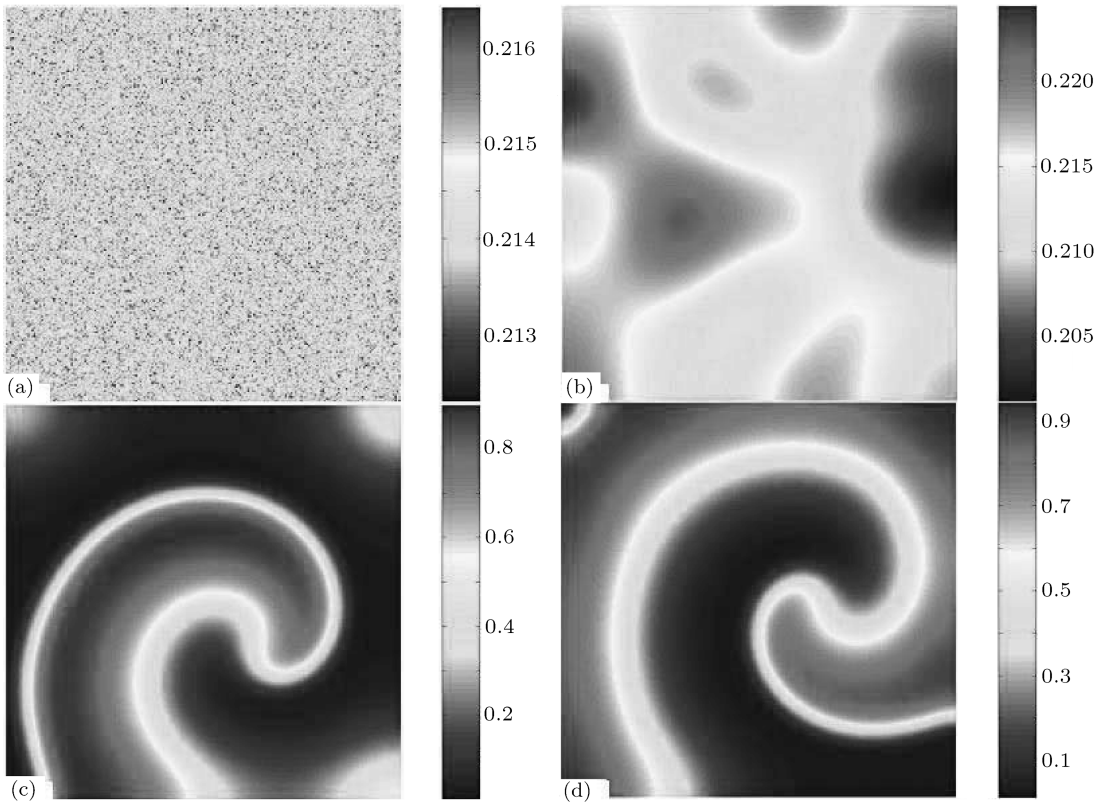


Fig. 6. Snapshots of contour pictures of the time evolution of the prey at different instants with $\alpha = 2.5$, $\beta = 1$, $\gamma = 8/9$, $\sigma = 0.7$: (a) $t = 0$; (b) $t = 50$; (c) $t = 500$; (d) $t = 5000$.

The above results are obtained from the initial condition considering the small spatial perturbation of the steady state E^* of the spatially homogeneous system. However, the type of the model dynamics depends on the choice of initial conditions.[6,23,24] In the following, we select a special perturbed initial condition[25] for investigating the evolution of the infected spatial pattern, the initial condition is introduced as

$$\begin{aligned} u(x,y,0) &= 1.0, \\ v(x,y,0) &= \begin{cases} 0.2, & \text{if} \quad (x-200)^2 + (y-200)^2 < 400, \\ 0, & \text{otherwise}, \end{cases} \end{aligned} \tag{15}$$

which is a circle. We adopt the parameter values as follows: $\alpha = 2.2$, $\beta = 1$, $\gamma = 8/9$, $\sigma = 0.05$, $\Delta h = 1/2$, $\Delta t = 1/24$, and $L = 200$. Then one can see that after a symmetrical target pattern, it grows slightly and the spots pattern (exterior) with target pattern (interior) emerges finally (c.f., Fig. 7). When σ increases to 0.075, more differently, we observe that after the decay of target patterns, the spots pattern prevails over the whole domain finally, and the dynamics of the system does not undergo any further changes (c.f., Fig. 8(d)).

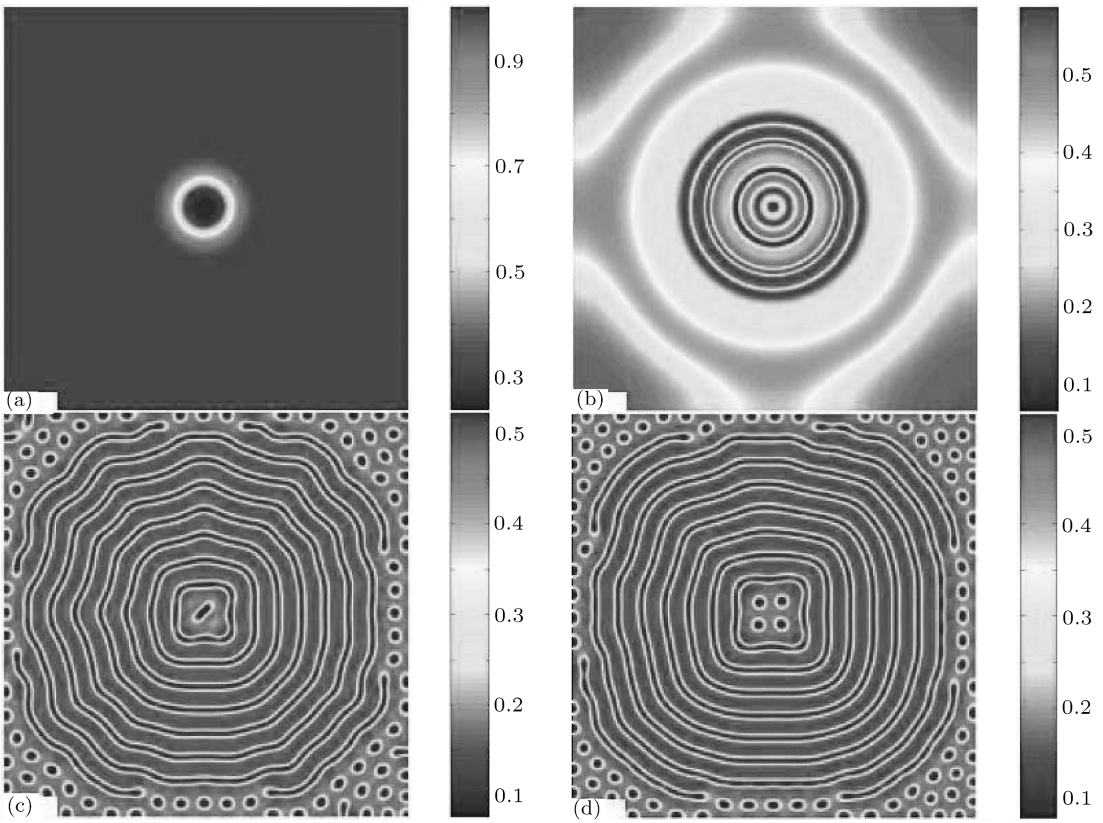


Fig. 7. Snapshots of contour pictures of the time evolution of the prey at different instants with $\alpha = 2.2$, $\beta = 1$, $\gamma = 8/9$, $\sigma = 0.05$: (a) $t = 5$; (b) $t = 100$; (c) $t = 4000$; (d) $t = 50000/3$.

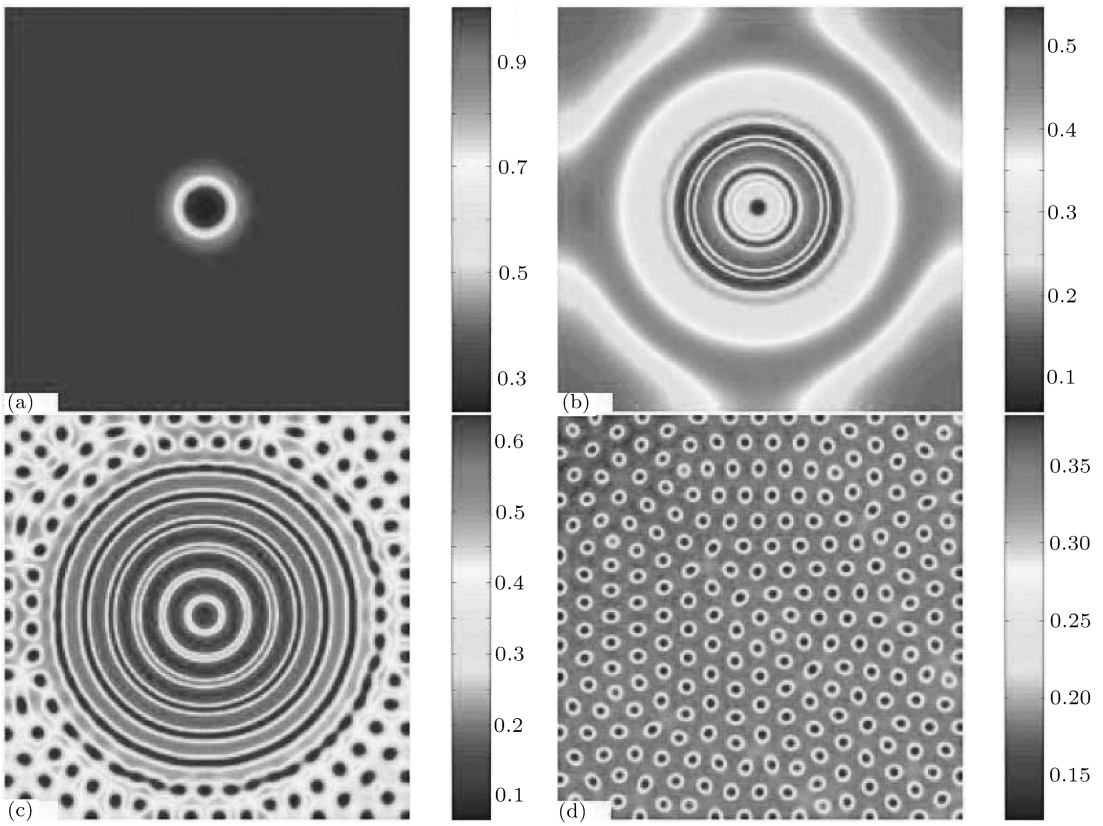


Fig. 8. Snapshots of contour pictures of the time evolution of the prey at different instants with with $\alpha = 2.2$, $\beta = 1$, $\gamma = 8/9$, $\sigma = 0.075$: (a) $t = 5$; (b) $t = 100$; (c) $t = 500$; (d) $t = 4000$.

5. Discussion

In this paper, the dynamic behaviour of a diffusive ratio-dependent predator–prey model within two-dimensional space is investigated. We observed that a non-trivial equilibrium point E^* exists for the model, and found that E^* is locally asymptotically stable when certain conditions are satisfied. Moreover, it has been shown that the instability observed in the model is diffusion-driven under the condition Eq. (14). It indicates the destabilisation of the homogeneous distribution of predator and prey and the emergence of spatial pattern formation phenomena.

Our analysis and numerical simulations reveal that the evolutionary process depends on several parameters. We find that different patterns appear on account of the change of α and σ. We also find that different initial conditions lead to different patterns. The biological implication of these results is that, in the absence of external influences, certain initial conditions can lead to spatial and temporal variations in densities of the populations that persist indefinitely.[24] For instance, experiments testing particular hypotheses could be performed in meso- or microcosmos to study microscale structure of planktonic spatial distributions. From our point of view, plankton pelagic communities are the best candidates in order to find empirical evidence with the least difficulty, although the mechanism should also operate in other aquatic and terrestrial systems.[21]

Our study shows that the model Eq. (2) represents rich spatio-temporal patterns, moreover, the existence of those patterns indicates that the diffusive ratio-dependent predator–prey model exhibits features which are not possible for the classical prey-dependent model,[21] Therefore, we hope that the results presented here will help to better understand the dynamic complexity of ecosystems.

References

[1] Turing A M 1952 *Philos. Trans. R. Soc. London* B **237** 37
[2] Ouyang Q and Swinney H L 1991 *Nature* **352** 610
[3] Li C P and Shen K 2003 *Chin. Phys.* **12** 184
[4] Gao Z Y and Lu Q S 2007 *Chin. Phys.* **16** 2479
[5] Sun G Q, Jin Z, Liu Q X and Li L 2008 *Chin. Phys.* B **17** 3936
[6] Medvinsky A B, Petrovskii S V, Tikhonova I A, Malchow H and Li B L 2002 *Siam. Rev.* **44** 311
[7] Wang W, Liu Q X and Jin Z 2007 *Phys. Rev.* E **75** 051913
[8] Zhang L, Wang W and Xue Y 2009 *Chaos, Solitons and Fractals* **41** 38
[9] Fan Y H, Li W T and Wang L L 2004 *Nonlinear Analysis: Real World Applications* **5** 247
[10] Hsu S B, Hwang T W and Kuang Y 2001 *Journal of Mathematical Biology* **42** 489
[11] Kuang Y 1999 *Differential Equations with Applications to Biology* **21** 325
[12] Xiao D and Li W 2003 *Proceedings of the Edinburgh* B *Mathematical Society* **46** 205
[13] Xu R, Chaplain M A J and Davidson F A 2004 *Applied Mathematics and Computation* **158** 729
[14] Berezovskaya F, Karev G and Arditi R 2001 *Journal of Mathematical Biology* **43** 221
[15] Fan Y H and Li W T 2004 *Journal of Mathematical Analysis and Applications* **299** 357
[16] Liu X X and Huang L H 2009 *Applied Mathematical Modelling* **33** 683
[17] Wang L L and Li W T 2004 *Journal of Computational and Applied Mathematics* **162** 341
[18] Matsuda H and Katsukawa T 2002 *Fisheries Oceanography* **11** 366
[19] Ahmad S and M R M Rao 1999 *Theory of Ordinary Differential Equations: with Applications in Biology and Engineering* (New Delhi: East-West Press) 50
[20] Murray J D 2003 *Mathematical Biology* (New York: Springer) 68
[21] Alonso D, Bartumeus F and Catalan J 2002 *Ecology* **83** 28
[22] Yang L and Epstein I R 2003 *Phys. Rev. Lett.* **90** 178303
[23] Garvie M R 2007 *Bulletin of Mathematical* **69** 931
[24] Sherratt J A, Eagan B T and Lewis M A 1997 *Philosophical Transactions: Biological Sciences* **352** 21
[25] Wang W, Zhang L, Wang H and Li Z 2008 arXiv:0801.0796